Comprehensive Tool Wear Estimation in Finish-Machining via Multivariate Time-Series Analysis of 3-D Cutting Forces

Y. Yao, X. D. Fang, G. Arndt (1); The University of Wollongong/Australia
Received on January 15, 1990

SUMMARY

In finish-machining, geometric accuracy and surface quality are adversely affected by the tool wear at the minor flank and nose area. This paper describes an investigation into "comprehensive" tool wear estimation, including flank-, crater-, minor flank-, and nose-wear, based on an analysis of dynamic cutting force in oblique machining. The force, measured in terms of its three orthogonal components, was used to develop trivariate Autoregressive Moving Average Vector (ARMAV) time series models. Based on these, dispersion analysis (DA) was used to extract features sensitive to the rate of various types of wear. The results show that minor flank wear reaches a critical value first in finish-machining, so that optimum cutting conditions or an appropriate tool change strategy must be determined on the basis of minor flank wear. The results also show that the method is a feasible means for on-line tool wear monitoring in finish-machining.

KEY WORDS: Multivariate Time-Series, Tool Wear, Dispersion Analysis, Finish-Machining, Minor Flank Wear, Nose Wear.

1. INTRODUCTION

The necessity of effective tool wear estimation in real-time has been recognized in relation to the needs of adaptive control and efficient tool change policy. Reported work has been concentrated on the estimation of flank wear [9,10,19] and some on flank and crater wear combined [1,7].

In operations such as a finish-turning of a bar, however, wear of the minor flank and nose plays a vital role in assuring the geometric accuracy and surface integrity of the finished product. It is obviously desirable for these wear states to be effectively monitored as well, because it is likely that wear in these areas may reach critical points earlier than those in the flank and crater, such that the optimum cutting conditions or tool change policy in a finish-operation have to be set based on these wear types. Therefore, a more comprehensive monitoring strategy involving multi-sensor or multi-modeling is called for.

Employing multi-sensor or multi-modeling strategies has been identified in a recent survey conducted for CIRP [17] as one of the three promising directions in machining process monitoring and control research. Interesting work has been reported in integrating force and acoustic emission (AE) signals via neural networks [14]. Chryssolouris [2] evaluated the effectiveness of sensor integration for tool wear estimation by neural network, least-squares regression, and the group method of data handling (GMDH) algorithm using simulation data. Both papers reported better estimation of flank wear by integrating multi-sensory information than by using a single sensor. For finish-machining where more than one quantity is to be estimated, however, a multi-sensor and multi-modeling strategy as suggested in [17] becomes necessary.

The "comprehensive" monitoring strategy has been addressed less frequently, perhaps because of the complexity of the machining process. If more than one quantity is to be estimated, more complexity will be encountered. This places higher demands on signal processing and analysis techniques which shall be able to "single out" from the signals particular ingredients sensitive to particular quantities to be estimated. Otherwise, multi-sensory techniques will do more harm than help. The spectrum analysis is a technique commonly used to single out frequency components to be correlated to tool wear [3,8,15]. Time domain methods, such as using autocorrelation coefficients of cutting force signals have been reported [19]. It, however, has been recognized that the cutting process is a stochastic process due to the existence of inevitable material property variations and other uncertainties. The necessity of employing stochastic analysis for cutting dynamics was emphasized in [6]. Interesting work on correlating coefficients of Autoregressive (AR) models of AE signals to the flank wear was reported [9], though appreciation of the results is impaired by inadequate physical interpretations. Another example of using stochastic analysis is to detect tool breakage by monitoring the residuals of an AR model obtained from cutting torque signals [16]. The residual analysis has been proven to be very effective to detect abrupt changes in the cutting process, such as tool breakage.

This paper describes an investigation into a comprehensive estimation strategy, including the rate of flank, crater, minor flank and nose wear, for oblique finish-turning operations of a bar. The estimation is based on the cutting force measured in terms of its three orthogonal components, from which trivariate Autoregressive Moving Average Vector (ARMAV) models [11] were developed. The dispersion analysis (DA) based on the ARMAV models [4,5] led to the discrimination between various modes of force variations in a quantitative way, such that correlating them to various quantities to be estimated was made possible. The correlation results were supported by physical interpretations.

2. TRIVARIATE ARMAV TIME SERIES MODELS FOR TOOL WEAR ESTIMATION

It is known that the dynamic cutting force, which is the variation from the average cutting force, contains richer information about tool/workpiece interactions during machining than the latter alone [6]. It has been shown that the dynamic cutting force is a stochastic signal which roughly obeys the normal distribution [18]. It is also appropriate to regard the dynamic force as stationary processes at different stages of wear development, because it takes only a fraction of a second for a set of a few hundred data points to be sampled each time. In summary, it is appropriate to apply statistical methods for stationary normal processes to the dynamic cutting force signal. As a way of analyzing the dynamics in the cutting force measurements, trivariate time series models, developed from the data, are used, since they give a concise parametric representation of the signals.

When a dynamic cutting force represented by its three orthogonal components is sampled at uniform intervals, Δ, the resulting discrete series of observation vectors; X_t, t=1, 2, ..., N; can be represented by

$$X_t = \sum_{i=1}^{n}\phi_i X_{t-i} + a_t - \sum_{i=1}^{m}\theta_i a_{t-i} \tag{1}$$

where the 3-dimensional vector of process variables is given by $X_t = [X_{1t}, X_{2t}, X_{3t}]^T$, $a_t = [a_{1t}, a_{2t}, a_{3t}]^T$, and $E[a_t a_{t-k}^T] = \delta_k \sigma_a$. Superscript T denotes vector transpose, E expectation, δ_k the Kronecker delta function, σ_a the covariance of a_t.

The model in Eq.1 is termed as Autoregressive Moving Average Vector model of autoregressive order n and moving average order m denoted by ARMAV(n,m). Such a model expresses the observed trivariate series, $X_{1t} = F_{xt}$ = feed force, $X_{2t} = F_{yt}$ = thrust force, and $X_{3t} = F_{zt}$ = main cutting force, as linear combinations of past observation vectors and independent random vectors a_t. The parameter matrices ϕ_i's and θ_i's are estimated based on the observation vectors and therefore describe instantaneous dynamics of the cutting process. The orders of an adequate model can be determined by the F-test or by examining the correlations of the independent random vectors a_t [11].

Once an adequate ARMAV model is determined, the Dispersion Analysis (DA) is carried out as follows. The characteristic parameter matrices, ϕ_i's, of the time series model given by Eq.1 are adjoined so that

$$T\Lambda T^{-1} = \begin{bmatrix} \phi_1 & \phi_2 & \cdots & \cdots & \phi_n \\ I & 0 & \cdots & \cdots & 0 \\ \cdots & \cdots & \cdots & \cdots & \cdots \\ 0 & \cdots & 0 & I & 0 \end{bmatrix} \tag{2}$$

where Λ is a matrix of eigenvalues and T the eigenvectors. It can be shown [11] that the correlation matrix of the measured variables is a weighted linear combination of the eigenvalues, λ_i, i=1,2, ..., 3n, as follows

$$\gamma_k = E[X_t X_{t-k}^T] = \sum_{i=1}^{3n} d_i \lambda_i^k \tag{3}$$

If k = 0, one obtains the covariance or dispersion matrix for the measured variables as

$$\gamma_0 = E[X_t X_t^T] = \sum_{i=1}^{3n} d_i \tag{4}$$

where d_i is the dispersion associated with eigenvalue λ_i and given by

$$d_i = \sum_{j=1}^{3n} \frac{g_i \sigma_a g_j^T}{1 - \lambda_i \lambda_j} \tag{5}$$

and g_i the products of submatrices of T and T^{-1}.

The significance of Eq.4 lies in the fact that the process variation γ_0 is decomposed into contributions of process eigenvalues in terms of dispersion d_i's quantitatively. Of particular interest are the d_i's associated with eigenvalues occurring in complex conjugate pairs which contribute to the oscillating or periodical variation of the process. The frequency corresponding to a pair of complex conjugate eigenvalues is given by

$$f_i\,(\mathrm{Hz}) = \frac{1}{2\pi\Delta}\tan^{-1}(\mathrm{Im}(\lambda_i)/\mathrm{Re}(\lambda_i)) \tag{6}$$

where Δ is the sample interval in seconds. By decomposing the process variation γ_0 into dispersion d_i's which correspond to eigenvalues and ultimately correspond to frequencies, an order of merit of the existing frequencies (oscillating modes) can be established such that analysis and interpretation in terms of physical phenomena, such as natural frequencies of the tool/tool holder system and machine tool structural frequencies can be carried out in a quantitative manner.

3. EXPERIMENTS AND TOOL WEAR MEASUREMENTS

3.1 Description of Experiments

The tool wear experiments were carried out using a dynamometer (KISTLER Type 9257A). Table 1 gives the machining conditions used in the experiments.

Table 1 Machining Conditions Used in Tool Wear Experiments

Machine Tool	Colchester Mascot 1600 (9.3 KW)
Tool Insert Type	TNMA160408F (Carbide)
Tool Geometry	Rake Angle 0°, Inclination Angle -6°, Relief Angle 5°, Cutting Edge Angle 0°
Work Material	AISI4140 (HBN=275-320)
Workpiece Dimension	Length =1m and Diameter =100mm
Cutting Conditions	Group 1 : V=115m/min f=0.1mm/rev d=0.5mm Group 2 : V=145m/min f=0.1mm/rev d=0.5mm Group 3 : V=145m/min f=0.06mm/rev d=0.5mm
Cutting Fluid	No

To assure the experimental conditions being as close as possible to practical machining operations, the machining process was interrupted periodically with an increment in period of about 5 minutes under cutting condition Group 1 and 2.5 minutes under Groups 2 and 3. The tool was replaced by a fresh one at each interruption such that every tool remained in thermal continuity until it was replaced. Just before each tool replacement, a set of 524 data points was sampled for each channel and a typical record is shown is Fig.1. Therefore, the experimental results consist of 8 tools and 8 sets of data from each channel under Group 1, and 7 tools and 7 sets of data from each channel under Groups 2 and 3.

Before the dynamic cutting force in terms of its three orthogonal components were sampled into a multi-channel data acquisition system with a sample interval equal to 60 μs (about 16.7 KHz), low-pass filters with a cut-off frequency of 4 KHz were applied, considering the 4 KHz-natural frequency of the dynamometer.

3.2 Definition of Comprehensive Tool Wear Parameters and Their Measurement

Eight parameters were selected to describe the tool wear states as shown in Fig.2, primarily in accordance with CIRP tool wear terminology [13]. The eight tool wear parameters are roughly classified into three categories with respect to different tool faces, i.e., the major flank area (VB, KS & VG), crater area (KT, KB & KK) and minor flank area (VB' & N). Table 2 gives the measurement results for Group 1 by microscopy, and the tool wear developments for all three cutting conditions are plotted in Figs. 3 and 4.

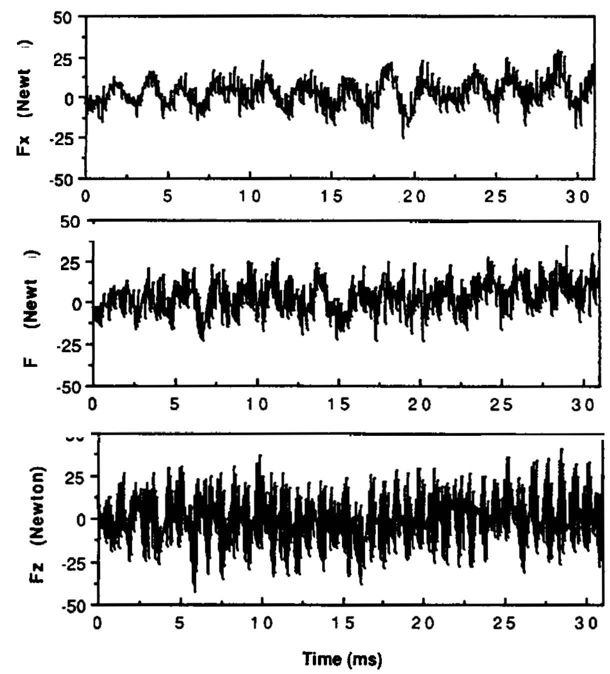

Fig. 1 Dynamic Cutting Force Measured in Terms of Its Three Orthogonal Components

Table 2 Tool Wear Measurement Results for Cutting Condition Group 1

Time (min)	VB (mm)	KS (μm)	VG (mm)	KT (μm)	KB (mm)	KK (mm)	VB' (μm)	N (μm)
0	0	0	0	0	0	0	0	0
2.67	0.12	12.8	0.09	22.2	1.1	0.4	15.3	7.1
5	0.16	25.7	0.10	33.3	1.2	0.60	28.6	21.4
10	0.26	47.1	0.40	38.8	1.2	0.63	71.4	32.8
15	0.34	80.0	0.70	66.7	1.2	0.64	185.7	54.3
20	0.58	104.3	0.75	166.7	1.4	0.66	228.6	91.4
25	0.64	127.1	0.80	205.6	1.4	0.68	235.7	112.8
34	0.73	142.8	0.84	222.2	1.5	0.70	242.8	135.7

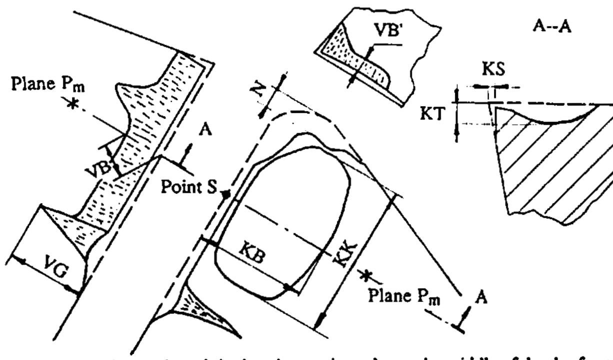

S : the point on the original major cutting edge at the middle of depth of cut
P_m: the plane perpendicular to the major cutting edge through point S

VB: major flank wear	VG: length of the groove (notch)
KS : retract of the cutting edge	KT : crater depth on the rake face
KB: crater width on the rake face	KK: crater length on the rake face
VB': minor flank wear	N : nose wear

Fig. 2 Definition of Comprehensive Tool Wear Parameters

4. TOOL WEAR ESTIMATION BY DISPERSION ANALYSIS

4.1 ARMAV Modeling and Dispersion Analysis

Each set of data was used to develop ARMAV models first. ARMAV(9,0) models were found adequate for data collected under cutting conditions denoted as Group 1 in Table 1 and ARMAV(11,0) models for the data collected under Group 2 and 3 conditions. Given below is an example of ARMAV(9,0) model.

$$X_t = \begin{bmatrix} .448 & -.063 & -.020 \\ .140 & .808 & -.018 \\ -.034 & .128 & .333 \end{bmatrix} X_{t-1} + \begin{bmatrix} -.129 & .115 & -.108 \\ -.063 & -.349 & -.062 \\ -.043 & -.083 & .265 \end{bmatrix} X_{t-2} + \begin{bmatrix} .262 & .013 & .193 \\ -.169 & .092 & .010 \\ .164 & -.060 & .052 \end{bmatrix} X_{t-3} +$$

$$\begin{bmatrix} .342 & -.023 & -.073 \\ .103 & -.034 & -.021 \\ -.085 & .105 & .048 \end{bmatrix} X_{t-4} + \begin{bmatrix} .187 & -.001 & .005 \\ -.162 & .188 & .088 \\ -.061 & -.054 & .047 \end{bmatrix} X_{t-5} + \begin{bmatrix} .018 & .059 & .099 \\ .084 & -.058 & -.045 \\ .004 & .011 & -.105 \end{bmatrix} X_{t-6} +$$

$$\begin{bmatrix} -.200 & -.161 & .010 \\ .035 & -.021 & -.016 \\ -.108 & .054 & .179 \end{bmatrix} X_{t-7} + \begin{bmatrix} -.086 & .158 & -.028 \\ .054 & -.064 & -.035 \\ .086 & -.161 & -.131 \end{bmatrix} X_{t-8} + \begin{bmatrix} -.084 & -057 & -.010 \\ -.003 & .012 & .105 \\ -.044 & .060 & -.003 \end{bmatrix} X_{t-9} + a_t$$

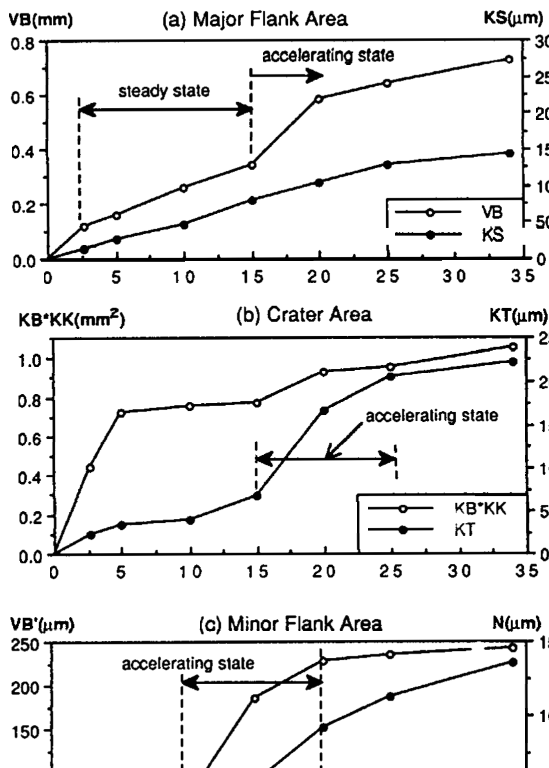

Fig. 3 Comprehensive Tool Wear Results for Cutting Condition Group 1 (V=115m/min, f=0.1mm/rev, d=0.5mm)

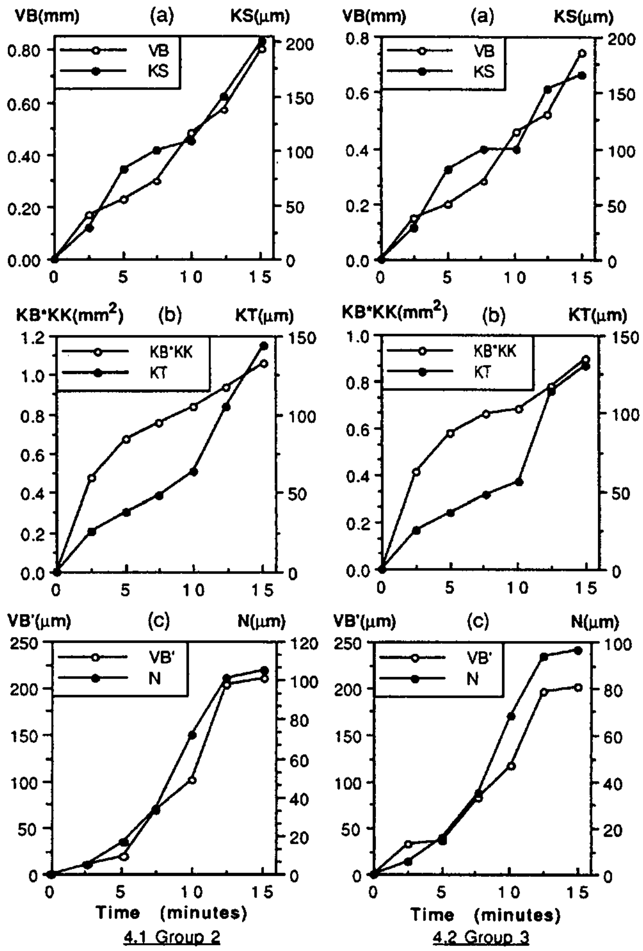

Fig.4 Comprehensive Tool Wear Results for Cutting Condition Groups 2 & 3

After an adequate model was determined, dispersion d_i's and corresponding frequencies were calculated according to Eqs. 5 and 6. The dominant d_i's (e.g. ones with larger percentage) and associated frequencies under cutting condition Group 1 are tabulated in Table 3. It is seen that the most significant dispersions are associated with a lower frequency (LF) range, and the second most significant dispersions related to a higher frequency (HF) range. The dominant dispersions for all three cutting conditions are plotted in Figs. 5 and 6, from which recognizable trends are observed which will be exploited in the following section.

Table 3 Dominant Dispersions (%) for Group 1

	Feed Force F_x		Thrust Force F_y		Main Cutting Force F_z	
Time (min)	LF (500-550 Hz)	HF (3.4-3.5 KHz)	LF (650-750 Hz)	HF (3.3-3.5 KHz)	LF (950-1050 Hz)	HF (2.6-2.8 KHz)
0	98.28	1.35	55.43	12.11	50.20	0.80
2.67	89.37	7.28	44.66	13.42	46.22	2.53
5	72.77	16.79	61.60	14.77	65.4	6.50
10	63.96	38.25	79.84	16.22	70.70	11.23
15	65.14	11.68	76.43	20.80	77.49	8.53
20	82.90	9.21	72.39	21.90	85.85	2.70
25	87.74	8.80	61.98	31.74	80.00	0.01
34	60.00	20.83	74.32	20.32	59.17	5.36

4.2 Analysis Associated with Physical Interpretation

Feed Direction: For an oblique turning operation of a bar, it is known that the feed force F_x is primarily associated with the normal force acting on the major flank $F_{\alpha n}$ and the horizontal friction force acting on the minor flank $F_{\beta h}$ (Fig.7). Therefore, the tool/workpiece interactions on both flanks should be reflected in the dynamic feed force characteristics.

By examining the trend of LF dispersions of 500-550Hz shown in Fig.5(a), it is found that the percentage values decrease to a minimum between 10 to 15 minutes (major flank wear VB = 0.35 mm), after which they increase. It is well known from experience that cutting tools are replaced or changed when the major flank wear reaches the critical values of 0.25-0.38 mm [10]. Beyond this critical wear, the rate of wear increases very rapidly, below it the rate first decreases and then becomes constant. Thus, the behaviour of the LF dispersions isolated from the dynamic feed force is very similar to the well-known rate of major flank wear curves and could be used as a good indicator for major flank wear.

By comparing the HF dispersion curve of 3.4-3.5 KHz shown in Fig.5(a) with the minor flank wear, VB' curve shown in Fig.3(c), it is again found the former resembles the slope (rate) of the latter. The acceleration of VB' at about 10 minutes could be detected by the maximum value of the HF dispersions.

Thrust Direction: The dynamic thrust force F_y mainly reflects the tool/workpiece interactions on both the rake face and the minor flank. The small depth of cut used in finish-machining produces a large chip flow angle such that the rake face

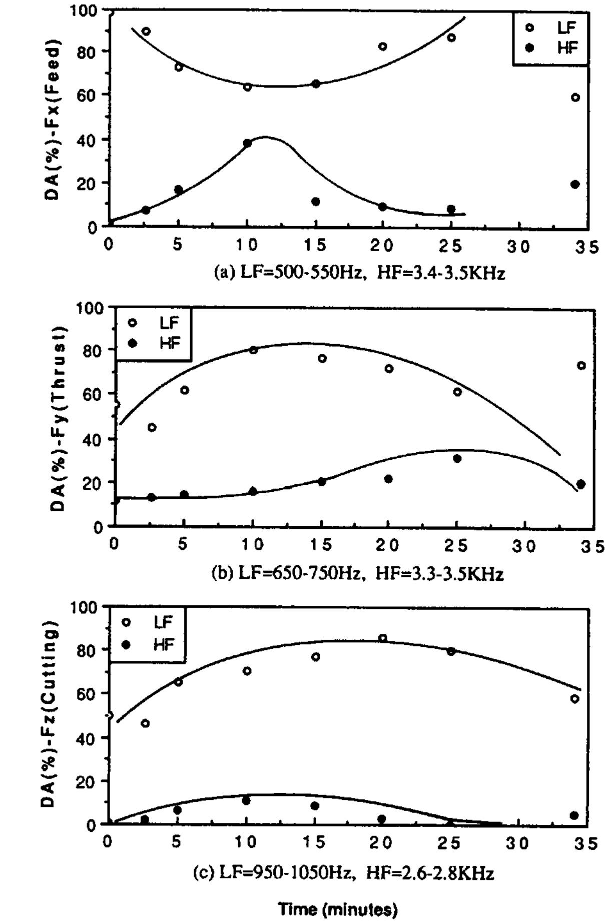

Fig. 5 Dispersion Diagram for Cutting Condition Group 1

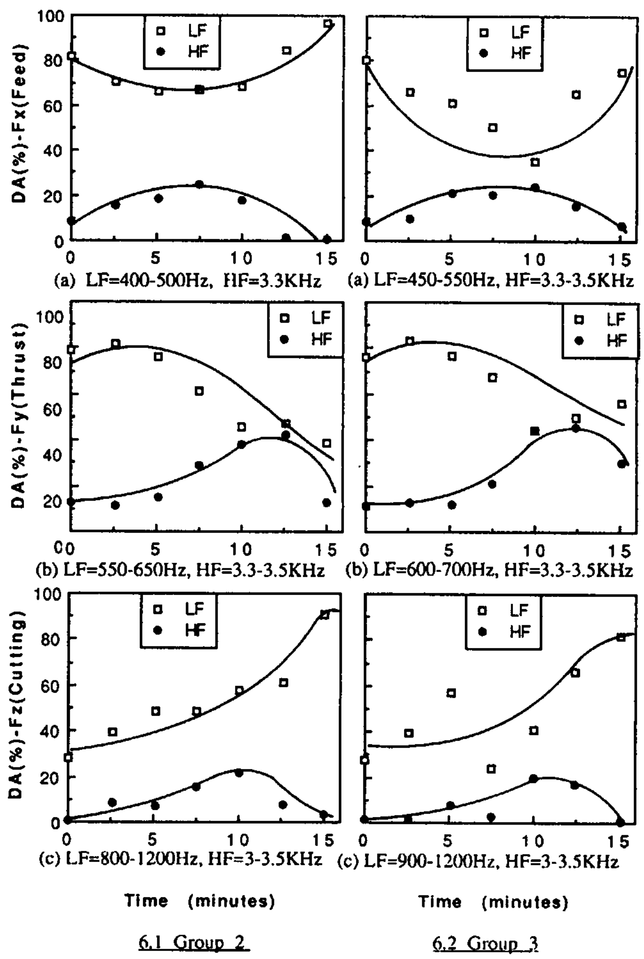

Fig. 6 Dispersion Diagrams for Cutting Condition Groups 2 & 3

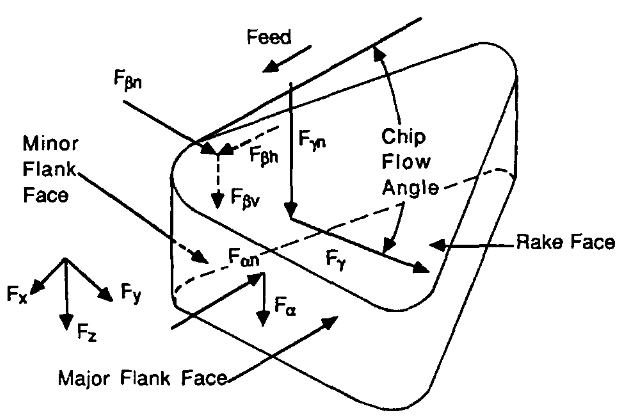

Fig. 7 Nomenclature Summary of the Forces Acting on Different Tool Faces

friction force F_y is almost along the y direction. The normal force acting on the minor flank $F_{\beta n}$ is also associated with F_y. In a similar manner, the HF dispersions of 3.3-3.5 KHz shown in Fig.5(b) can be related to the rate of crater wear KT shown in Fig.3(b), and the LF dispersions of 650-750 Hz shown in Fig.5(b) related to the rate of the minor flank wear VB' shown in Fig.3(c). Therefore, they can be used for minor flank and crater wear monitoring purposes.

Cutting Direction: The dynamic cutting force F_z is primarily associated with the normal force acting on the rake face $F_{\gamma n}$, the friction force acting on the major flank F_{α}, and the vertical friction force on the minor flank $F_{\beta v}$. By examining the LF and HF dispersions of 950-1050 Hz and 2.6-2.8 KHz shown in Fig.5(c), it was found that they reflect the rate of the rake wear and the minor flank wear shown in Figs.3(b) and 3(c), respectively.

As summarized in Table 4, the trends of the LF dispersions isolated form all three components of the dynamic cutting force reflect the wear rate mechanism associated with normal forces, and the HF dispersions reflect the wear rate mechanism associated with tangential (friction) forces. Similar results were obtained for experiments under cutting condition Groups 2 and 3 as shown in Figs. 4 and 6.

Table 4 Tool Wear Analysis for Cutting Condition Group 1

F_x	$F_{\alpha n}$	(Normal to Major Flank)	↔	VB, KS	↔	LF Dispersions (500-550 Hz)
	$F_{\beta h}$	(Tangential to Minor Flank)	↔	VB', N	↔	HF Dispersions (3.4-3.5 KHz)
F_y	$F_{\beta n}$	(Normal to Minor Flank)	↔	VB', N	↔	LF Dispersions (650-750 Hz)
	F_{γ}	(Tangential to Crater Face)	↔	KT	↔	HF Dispersions (3.3-3.5 KHz)
F_z	$F_{\gamma n}$	(Normal to Crater Face)	↔	KT	↔	LF Dispersions (950-1050 Hz)
	$F_{\beta v}$	(Tangential to Minor Flank)	↔	VB', N	↔	HF Dispersions (2.6-2.8 KHz)
	F_{α}	(Tangential to Major Flank)				

5. DISCUSSION

5.1 Critical Tool Wear in Finish-Machining and Sensing Strategy

It is clear from the above results that the HF dispersion of F_x, the LF dispersion of F_y, and the HF dispersion of F_z can all be used as indicators of the rate of minor flank wear VB'. They all reached a maximum value when VB' accelerated at about 10 minutes under cutting condition Group 1. Among them the most sensitive one is the HF dispersion of F_z. The horizontal friction force on the minor flank, $F_{\beta h}$, which has been shown to be associated with the HF dispersion of F_x, is more a static than a dynamic one, because of the slow feed motion. The LF dispersion of F_y is also relatively less sensitive due to the fact that there is no feeding motion in the thrust direction. Therefore, HF dispersion of F_z can be used as the main indicator of the minor flank wear VB', and the other two as auxiliary ones. When one or more of them reaches the maximum, the accelerated minor flank wear is indicated.

In comparison to major flank and crater wear, both of which did not reach their critical points until after about 15 minutes under cutting condition Group 1, it becomes obvious that for operations such as a finish-turning of a bar, the adaptive control and effective tool change policy has to be set based on the wear states of the minor flank area, to assure geometric accuracy and surface quality of the finished workpiece.

5.2 Structural Dynamics and Idle Disturbances

Clear patterns linking the force variations in terms of dispersions and associated frequencies, isolated from dynamic cutting force, to the various wear development rates have been identified. However, the physical nature of the relationships is unclear and it is the purpose of this section to identify physical origins of these relationships and interpret accordingly.

Since almost the same HFs appear in all three groups, these frequencies are then inherent in the tool holder and hence may be conjectured to relate to its natural frequencies. Tests revealed that the natural frequencies of the tool holder/dynamometer system were 3320 Hz in the x-, 3300 Hz in the y-, and 2847 Hz in the z- directions, respectively. These values match reasonably well with the HF's isolated from the dynamic cutting force (Figs.3 and 4).

Tests on dynamometer frequency response to idle speed excitation alone revealed idle frequencies of 575 Hz for x, 715 Hz for y, and 975 Hz for z under cutting condition Group 1. These frequencies are reasonably close to the LF's listed in Table 3. From the above tests, it becomes clear that tool/workpiece interaction at the LF's are related to the idle frequencies, and the HF's are mainly associated with the natural frequencies of the tool-holder/dynamometer system.

6. CONCLUSIONS

1. Dispersion analysis based on trivariate ARMAV time series models was used to quantitatively decompose the dynamic cutting force in terms of dispersions (relative importance of modes of force variation) and associated frequencies. The merit of the method is its ability to isolate from the dynamic cutting force the ingredients, each of which is particularly sensitive to a particular wear state, thereby providing much more comprehensive yet sensitive estimates than those possible by using the force signal in a lump-sum manner.

2. The patterns of change of the dispersions resemble the rate of various wear parameters and the resemblance is physically interpreted. The rapidly increasing rate of the minor flank wear occurring before the accelerating stage of the major flank wear is due to the fact that the gradually increasing major flank wear, and retreat of the cutting edge, sharpens the nose and puts more burden on the minor flank and edge, to a point where drastic minor flank wear is inevitable. Therefore, for operations such as a finish-turning of a bar, optimum cutting conditions or effective tool change strategy have to be determined based on the minor flank wear instead of others, to assure geometric accuracy and surface quality of the finished workpiece.

3. It was the purpose of this investigation to establish relationships between the off-line measurements of wear and dispersions of dynamic force measurements, such that the latter alone will be capable of predicting wear on-line. For machining processes at normal speeds, the algorithm introduced above is sufficiently fast to determine wear states in real time. For processes with a higher speed, the algorithm could be readily reformulated into a recursive one such that faster wear developments can be traced.

ACKNOWLEDGEMENT

The authors gratefully acknowledge partial supports from the Australian Research Council and the University of Wollongong Research Grant Scheme.

REFERENCES

1. Chryssolouris, G., Guillot, M. and Domroese, M., 1987, Tool Wear Estimation for Intelligent Machining, ASME/WAM, Intelligent Control, DSC - Vol. 5, pp 35-43.
2. Chryssolouris, G. and Domroese, M., 1988, Sensor Integration for Tool Wear Estimation in Machining, ASME/WAM, Sensors and Controls for Manufacturing, PED - Vol. 33, pp 115-123.
3. Del Taglia, A., et. al., 1976, An Approach to On-line Measurement of Tool Wear by Spectrum Analysis, Proc. of Int. Machine Tool Design and Research Conf., pp 141-148.
4. DeVries, W.R., Dornfeld, D.A., and Wu, S.M., 1978, Bivariate Time Series Analysis of the Effective Force Variation and Friction Coefficient Distribution in Wood Grinding, ASME Trans., J. of Engineering for Industry, May 1978, Vol. 100, pp 181-185.
5. DeVries, W.R., and Wu, S.M., 1978, Evaluation of Process Control Effectiveness and Diagnosis of Variation in Paper Basis Weight via Multivariate Time-Series Analysis, IEEE Trans. Automatic Control, Vol. AC - 23, No. 4, pp 702-708.
6. Eman, K.F., and Wu, S.M., 1987, Present and Future Trends in Stochastic Analysis of Cutting and Structural Dynamics, 15th NAMRC, pp 426-432.
7. Giusti, F., Santochi, M., and Tantussi, G., 1987, On-Line Sensing of Flank and Crater Wear of Cutting Tools, Annals of the CIRP, Vol. 36/1, pp 41-44.
8. Jiang, C.Y., Zhang, Y.Z. and Xu, H.J., 1987, In-Process Monitoring of Tool Wear Stage by the Frequency Band-Energy Method, Annals of the CIRP, Vol. 36/1, pp 45-48.
9. Liang, S.Y., and Dornfeld, D.A., 1987, Detection of Cutting Tool Wear Using Adaptive Time Series Modeling of Acoustic Emission Signal, ASME/WAM, Sensors for Manufacturing, PED - Vol. 26, pp. 27-38.
10. Pandit, S.M., and Kashou, S., 1982, A Data Dependent Systems Strategy of On-line Tool Wear Sensing, ASME Trans., J. of Engineering for Industry, August 1982, Vol. 104, pp 217-223.
11. Pandit, S.M., and Wu, S.M., 1983, Time Series and System Analysis with Applications, John Wiley.
12. Pandit, S.M., and Kashou, S., 1983, Variation in Friction Coefficient with Tool Wear, Wear, Vol. 84, pp 65-79.
13. Pekelaring, A.J., and Van Luttervelt, C.A., CIRP Terminology and Procedures for Turning Research.
14. Rangwala, S., and Dornfeld, D., 1987, Integration of Sensors via Neural Networks for Detection of Tool Wear States, ASME/WAM, Intelligent and Integrated Manufacturing Analysis & Synthesis, PED - Vol. 25, pp 109-120.
15. Sata, T., et. al, 1973, Learning and Recognition of the Cutting States by the Spectrum Analysis, Annals of the CIRP, Vol. 22/1, pp 41-42.
16. Takata, S., and Sata, T., 1986, Model Referenced Monitoring and Diagnosis - Application to Manufacturing System, Computers in Industry, 7, pp 31-43.
17. Toenshoff, H.K., Wulfsberg, J.P., Kals, H.J.J., and Koenig, W., 1988, Developments and Trends in Monitoring and Control of Machining Processes, Annals of the CIRP, Vol. 37/2, pp 611-622.
18. Wu, B., et. al., 1987, The Dynamic Component of Cutting Force and its Application in Cutting State Identification, J. of Nanjing Institute of Technology, Vol. 17, No. 6 (I), pp 55-65.
19. Yuan, Z.J., et. al., 1988, In-Process Detection of Tool Wear and Breakage by Autocorrelation Coefficient of Dynamic Cutting Forces in Turning, Proc. 4th Int. Conf. on Manufacturing Engineering, Brisbane, Qld, Australia, May 11-13, pp 201-205.